

## SURFACE ENGINEERING OF CDS/ZNS QDS VIA GLUTATHIONE CAPPING: FTIR AND COLLOIDAL STABILITY ASSESSMENT

Rama Siripelly<sup>1</sup>, P.Pushpalatha<sup>2</sup>, Budida Latha<sup>3</sup>, Pavithra Dasari<sup>4</sup>, Anupalli Roja Rani\*

Department of Biotechnology, University College of Science, Osmania University,  
Hyderabad-5000 007, Telangana, India.

\*Corresponding Author

Email: anupallirr@gmail.com

### Abstract

*This study examines the aqueous-phase ligand exchange of hydrophobic CdS/ZnS core-shell QDs utilizing reduced glutathione (GSH) and assesses their physicochemical stability across different solvent and pH conditions. A biphasic ligand exchange technique was utilized to substitute Trioctylphosphine oxide ligands with glutathione, making the QDswater dispersible. Fourier-transform infrared spectroscopy validated thiol-metal coordination and surface functionalization with glutathione. Dynamic light scattering demonstrated an increase in hydrodynamic diameter from around 7.4 nm to about 11.2 nm post-exchange, while zeta potential studies indicated improved colloidal stability at -26.3 mV. Stability experiments exhibited superior optical and colloidal performance in Milli-Q water and phosphate-buffered saline, with modest aggregation observed in protein-rich environments. The pH-responsive behaviour demonstrated excellent stability throughout the range of pH 7.0 to 8.0. These findings confirm GSH as a potent ligand for stabilizing QDs in aquatic environments, endorsing their applicability in biological and diagnostic fields.*

**Keywords:** CdS/ZnS QDs, colloidal stability, glutathione capping, ligand exchange, pH-dependent behaviour, surface charge

### 1. Introduction

Semiconductor quantum dots (QDs) have become a crucial category of nanomaterials in optical imaging, biosensing, and diagnostics because of their distinctive photophysical characteristics (Martynenko et al. 2017). In

contrast to traditional fluorophores, QDs have numerous advantages, such as extensive absorption spectra, narrow and adjustable emission peaks, elevated quantum yields, and enhanced photostability. These characteristics make them especially appealing for aqueous-phase applications, including bioimaging, drug administration, and molecular tracking in intricate biological settings. Nonetheless, the actual use of QDs in aquatic or physiological systems is a significant difficulty, chiefly due to their intrinsic surface chemistry (Mondal et al. 2024).

Generally, as-synthesized QDs are coated with hydrophobic ligands such as Trioctylphosphine oxide (TOPO), oleic acid, or hexadecyl amine to ensure their stability in organic solvents (Shao et al. 2011). Although efficient for colloidal control during synthesis, these ligands significantly restrict QD dispersibility in water and inhibit their direct application in biological systems. Furthermore, these hydrophobic surface coatings are susceptible to detachment in polar conditions, resulting in aggregation, fluorescence suppression, and cytotoxicity from heavy metal ion leaching. Consequently, surface modification techniques are essential to convert these

nanocrystals into stable, water-soluble, and biocompatible forms appropriate for biomedical and environmental applications(Amiri et al. 2025).

Ligand exchange is a prevalent method for substituting the natural hydrophobic ligands on quantum dot surfaces with hydrophilic, functional compounds. Among the capping agents, reduced glutathione (GSH) has garnered significant attention owing to its distinctive physicochemical and biological properties(Yadav and Preet 2023). GSH is a naturally occurring tripeptide consisting of thiol, amine, and carboxylic functional groups(Sahu et al. 2024). The thiol group demonstrates a significant attraction to the metal atoms on the quantum dot surface, facilitating secure anchoring via metal-thiolate interaction, while the other functional groups enhance water dispersibility, charge stability, and pH buffering. Moreover, the zwitterionic characteristics of GSH reduce nonspecific interactions and improve biocompatibility, rendering it an optimal ligand for the fabrication of QDs for physiological purposes(Yang et al. 2025).

Although GSH is extensively utilized in QD functionalization, the majority of current research has predominantly concentrated on the resultant photoluminescence or cellular absorption, frequently neglecting the essential factor of long-term colloidal and structural stability. Specifically, systematic studies evaluating the behaviour of GSH-capped QDs under varying solvent conditions and pH levels factors that simulate storage, handling, and physiological stress are

scarce. Comprehending stability patterns following ligand exchange is essential for optimizing quantum dot formulations for practical applications(Liao et al. 2019).

This study examines the aqueous-phase ligand exchange of pre-synthesized CdS/ZnS core-shell QDs with reduced glutathione and assesses their colloidal and chemical stability under physiologically relevant conditions. We evaluate the surface modification and analyse the behaviour of GSH-capped QDs in aqueous solutions with various pH values using Fourier-transform infrared spectroscopy (FTIR), dynamic light scattering (DLS), and zeta potential analysis. This study offers significant insights into the stability of GSH-based ligand engineering and its appropriateness for biological and environmental applications by creating a comprehensive stability profile following functionalization.

## 2. Materials and Methods

### 2.1. Chemicals and Reagents

Hydrophobic CdS/ZnS core-shell QDs were acquired from an in-house stock manufactured via standard organometallic hot-injection and successive ionic layer adsorption and reaction (SILAR) methods(Vyshnava et al. 2022). The QDs were initially coated with hydrophobic ligands, including Trioctylphosphine oxide (TOPO), oleic acid (OA), and hexadecyl amine (HDA), rendering them dispersible just in nonpolar solvents like chloroform.Reduced glutathione (GSH,  $\geq 98\%$  purity) was obtained from HiMedia (India) and utilized as the hydrophilic

ligand for surface modification in the aqueous phase. All additional chemicals, including chloroform ( $\geq 99.8\%$ ), sodium hydroxide (NaOH,  $\geq 98\%$ ), and phosphate-buffered saline (1X PBS), were of analytical quality and procured from Merck. All aqueous formulations utilized Milli-Q grade water (resistivity  $\geq 18.2 \text{ M}\Omega \cdot \text{cm}$ ). Dulbecco's Modified Eagle Medium (DMEM) supplemented with 10% foetal bovine serum (FBS) was procured from Gibco (USA) for stability assessment.

## 2.2. Ligand Exchange Protocol

The hydrophobic CdS/ZnS QDs were made water-dispersible using a biphasic ligand exchange process utilizing reduced glutathione. This approach involves mixing 1 mg of hydrophobic QDs distributed in 5 mL of chloroform with 5 mL of an aqueous glutathione solution (20 mM, pH adjusted to 8.0 using 0.1 M sodium hydroxide). The biphasic mixture was agitated vigorously at ambient temperature for 24 hours to promote the substitution of native ligands (OA, TOPO, HDA) with GSH via thiol-metal surface coordination.

Subsequent to the ligand exchange, the aqueous phase containing GSH-functionalized CdS/ZnS QDs was meticulously isolated and purified using centrifugation at 10,000 rpm for 10 minutes. The pellet was redispersed in Milli-Q water and subjected to three washes to eliminate unbound GSH and residual organic solvents. The resultant CdS/ZnS/GSH QDs manifested as a transparent, pale-yellow aqueous colloid

and were preserved at 4 °C in darkness until subsequent application. This approach was refined to preserve colloidal stability by maintaining an alkaline reaction mixture and employing an excess of glutathione to guarantee thorough surface passivation.

## 2.3. Characterization Techniques

Fourier-Transform Infrared Spectroscopy (FTIR) was employed to confirm the presence and attachment of GSH on the surface of the QDs. Lyophilized samples of unaltered and GSH-modified QDs were combined with anhydrous potassium bromide (KBr) and compressed into pellets. Spectra were obtained utilizing a Bruker Tensor II spectrometer across the range of 4000–400  $\text{cm}^{-1}$ . The hydrodynamic diameter and particle size distribution of QDs were assessed utilizing a Malvern Zetasizer Nano ZS at 25 °C. Measurements were conducted at a concentration of 0.1 mg/mL in phosphate-buffered saline (pH 7.4). The temporal evolution of size served as a metric for colloidal stability. Zeta potential was employed to evaluate surface charge and electrostatic stability. Measurements were conducted in Milli-Q water, PBS, and DMEM media to evaluate colloidal behaviour under varying ionic circumstances. All data were documented as the average of three separate trials and presented as mean  $\pm$  standard deviation.

## 2.4. Stability Testing

### 2.4.1. Solvent-Based Stability

To evaluate the impact of various aquatic environments, GSH-capped QDs were

suspended at a concentration of 0.1 mg/mL in Milli-Q water, 1X PBS, and full DMEM (including 10% FBS). Samples were preserved in amber vials at 25 °C for a duration of 7 days. DLS and zeta potential measurements were obtained at 0, 24, 72, and 168 hours to monitor alterations in hydrodynamic size and surface charge. All measurements were conducted in duplicate.

#### **2.4.2. Stability Dependent on pH**

For pH stability investigations, QDs were suspended in phosphate-buffered solutions with pH values varied from 4.0 to 9.0 in 0.5-unit increments using 0.1 M hydrochloric acid or sodium hydroxide. The specimens were incubated at 25 °C for a duration of 7 days. Stability was assessed by measuring hydrodynamic diameter and zeta potential on Day 0 and Day 7. An increase in particle size was read as aggregation, but a drop in zeta potential signified a loss of electrostatic stability or ligand desorption.

#### **2.5. Statistical Examination**

All experiments were conducted in triplicate unless specified differently. Data were presented as mean  $\pm$  standard deviation. One-way ANOVA, accompanied by Tukey's post hoc test, was employed for statistical comparisons, with significance established at  $p < 0.05$ . Data analysis was conducted using GraphPad Prism 8 software.

### **3. Results and Discussions**

#### **3.1. Ligand Exchange of CdS/ZnS QDs Utilizing Glutathione**

The conversion of hydrophobic QDs into water-dispersible nanostructures via surface ligand alteration is a crucial advancement for their utilization in biological and environmental applications. This study successfully transformed the surface chemistry of CdS/ZnS core-shell QDs by substituting their native hydrophobic ligands mainly TOPO, OA, and HDA with GSH. The replacement was executed by a biphasic ligand exchange method, involving the interaction of a chloroform solution containing hydrophobic QDs with an aqueous glutathione solution at an alkaline pH of 8.0. At this pH, the thiol group of GSH is in its deprotonated state, which amplifies its nucleophilic properties and promotes thiol-metal interaction with cadmium and zinc atoms at the QD surface. The process was influenced by the disparity in ligand binding affinities and the amphiphilic characteristics of GSH, enabling it to function as both a surface stabilizer and a solubilizing agent. Following 24 hours of intense agitation, a discernible phase transition from the organic to the aqueous phase was noted, signifying the effective substitution of hydrophobic ligands. The aqueous phase maintained the distinctive yellow coloration of QDs and displayed intense fluorescence under UV illumination, indicating that the core-shell architecture and optical integrity were intact following ligand exchange, as shown in **Fig 1**. This study enhanced the ligand exchange mechanism for stability by sustaining an excess of GSH and a mildly alkaline environment, assuring comprehensive surface coverage and reducing free surface states that could

result in aggregation or photoluminescence quenching (Bagherpour and Pérez-García 2024).

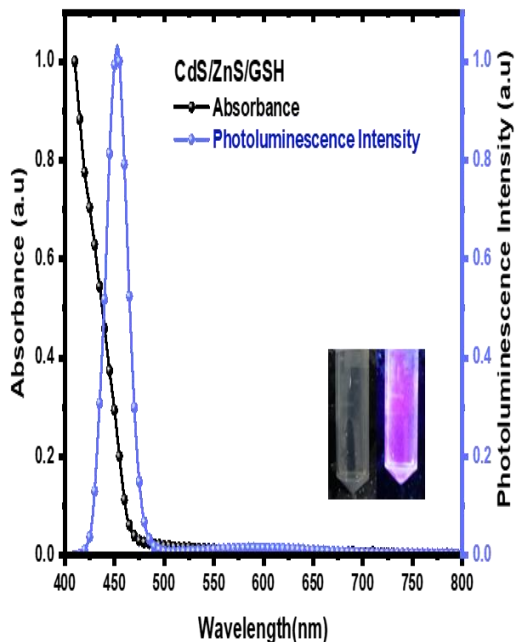


**Fig 1.** Fluorescence emission spectrum of GSH-capped CdS/ZnS QDs in aqueous media, retaining emission intensity and spectral features. Inset: Aqueous GSH-QDs under ambient (left) and UV (right) illumination, indicating retained luminescence post-ligand exchange

### 3.2. Verification of Ligand Functionalization by FTIR Spectroscopy

FTIR spectroscopy was utilized to verify the successful binding of GSH to the quantum dot surface. The FTIR spectrum of the GSH-capped QDs exhibited distinct vibrational bands indicative of glutathione, which were not present in the spectra of unmodified hydrophobic QDs. An extensive absorption band about  $3400\text{ cm}^{-1}$  was ascribed to the O–H and N–H stretching vibrations of hydroxyl and amine groups inside the glutathione backbone. Peaks at  $2925\text{ cm}^{-1}$  and  $2854$

$\text{cm}^{-1}$  correlate to C–H stretching vibrations of the aliphatic chains, as shown in Fig 2 (Chakrabarty et al. 2020).

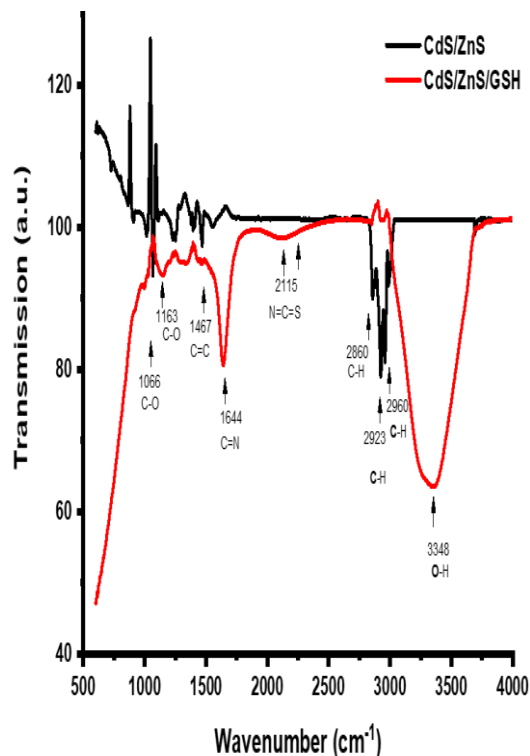


**Fig 2.** FTIR spectra of CdS/ZnS and CdS/ZnS/GSH quantum dots. The CdS/ZnS/GSH sample exhibits characteristic bands of glutathione, including –OH/NH stretching ( $\sim 3400\text{ cm}^{-1}$ ), amide I and II ( $\sim 1650$  and  $\sim 1540\text{ cm}^{-1}$ ), C–H stretching ( $\sim 2925$  and  $\sim 2854\text{ cm}^{-1}$ ), and C–S stretching ( $\sim 1070\text{ cm}^{-1}$ ), confirming successful surface functionalization through ligand exchange..

The distinct bands at approximately  $1650\text{ cm}^{-1}$  and  $1540\text{ cm}^{-1}$  corroborated the amide I (C=O stretching) and amide II (N–H bending and C–N stretching) modes, respectively, signifying the existence of the peptide bond backbone of GSH on the QD surface. The prominent peak at approximately  $1070\text{ cm}^{-1}$  was attributed to

C–S stretching, indicating metal–thiolate interaction and providing direct evidence of GSH binding to the QD surface via its thiol group. The lack of this peak in the unmodified QDs and its emergence in the functionalized sample validates the efficacy of the ligand exchange procedure (Wu et al. 2020). A symmetric  $\text{COO}^-$  stretch at around  $1400\text{ cm}^{-1}$  indicated the presence of deprotonated carboxylate groups that contribute to surface charge and electrostatic stability. The spectrum characteristics collectively confirm the covalent bonding of GSH to the QD surface, while preserving functional groups essential for colloidal stability and possible bioconjugation (Kaur et al. 2021).

### 3.3. Modification of Hydrodynamic Size and Dispersion Characteristics Assessed by DLS

DLS research yielded quantitative data regarding the hydrodynamic properties of the QDs post-glutathione capping (Jiang et al. 2021). Before ligand exchange, the hydrophobic QDs dispersed in nonpolar liquids displayed an average hydrodynamic diameter of roughly 7.4 nm, aligning with the core-shell dimensions established through transmission electron microscopy imaging, as shown in Fig 3. Subsequent to GSH functionalization and resuspension in aqueous solutions, the hydrodynamic diameter rose to around 11.2 nm. This augmentation is ascribed to the existence of the glutathione ligand shell and the adjacent hydration layer created by the polar functional groups of GSH in aqueous solution (Al-Barram 2021).

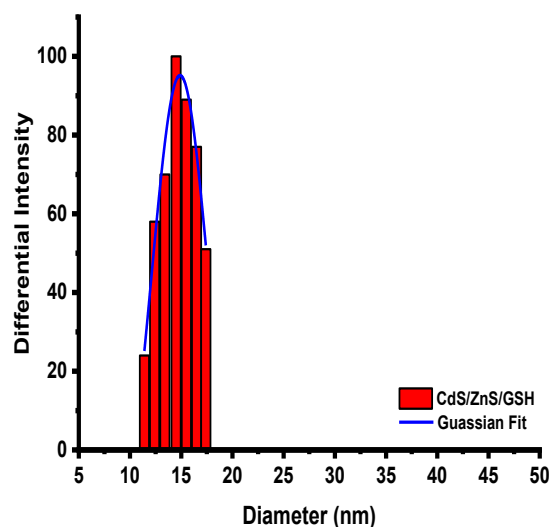


Fig 3. DLS of CdS/ZnS/GSH QDs showing increased size (~11.2 nm) after ligand exchange.

The noted increase in size does not indicate aggregation but rather signifies the enlargement of the effective hydrodynamic radius resulting from surface passivation and solvation. The polydispersity index (PDI) was low ( $<0.2$ ), indicating a restricted size distribution and steady colloidal dispersion. A little broadening in the size distribution histogram was noted, possibly resulting from temporary interparticle interactions facilitated by hydrogen bonding or electrostatic forces in the solution (Santos et al. 2016). This outcome aligns with the zwitterionic nature of glutathione and its capacity to form a hydrated shell, thereby augmenting steric and electrostatic stability. The DLS data indicate that ligand exchange with GSH results in well-dispersed, monodisperse QDs that maintain stability in water during short-term storage.

### 3.4. Augmentation of Surface Charge and Electrokinetic Stability via Zeta Potential

Zeta potential measurements provided essential insights into the electrostatic stability of the QDs following ligand exchange (Koo et al. 2011). The natural hydrophobic QDs, when dispersed in aqueous solutions, exhibited a zeta potential of -9.1 mV, signifying inadequate surface charge to avert aggregation under physiological or storage conditions. Conversely, GSH-functionalized QDs demonstrated a significantly higher negative zeta potential of -26.3 mV. The augmentation of surface charge is directly associated with the anionic functional groups (carboxylate and deprotonated thiol) inherent to the GSH molecule (Al-Barram 2021). A zeta potential magnitude exceeding  $\pm 25$  mV is typically regarded as adequate for the electrostatic stability of colloidal nanoparticles, as shown in Fig 4. The significant negative potential guarantees robust repulsive forces between particles, thus reducing aggregation caused by van der Waals attraction or Brownian motion. Measurements conducted in several solvents further validated the influence of medium ionic strength on electrokinetic stability. In Milli-Q water, the QDs exhibited a zeta potential of -26.3 mV, signifying optimal electrostatic stability. In PBS, the zeta potential diminished to -18 mV as a result of ionic screening by phosphate and sodium ions. In DMEM, which includes serum proteins and divalent cations, the zeta potential fell to around -12 mV, indicating partial charge neutralization and the potential creation of a protein corona. These data indicate that GSH capping substantially improves the colloidal stability of QDs in aqueous environments and retains

moderate efficacy even during ionic stress or biological simulation, as listed in Table 1 (Santos et al. 2016).

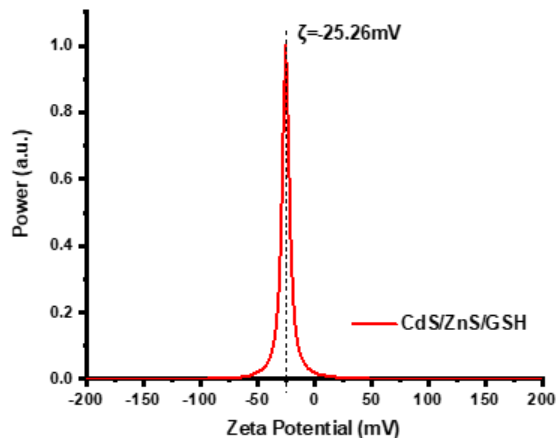


**Fig 4.** Zeta potential of CdS/ZnS/GSH QDs recorded at -25.2 mV, confirming enhanced colloidal stability after GSH capping.

**Table 1.** Properties of CdS/ZnS quantum dots before and after GSH modification

Property	Emission Wavelength (nm)	FWHM (nm)	Quantum Yield (%)	Hydrodynamic Size (nm)	Zeta Potential (mV)
CdS/ZnS QDs (Before GSH)	450	35	61	8.5	-22.3
CdS/ZnS-GSH QDs (After GSH)	452	38	45	11.8	-25.26

**3.4. Evaluation of Stability in Aqueous Solvents and Biological Environments**

The temporal colloidal and optical stability of QDs is essential for their practical use

in imaging, diagnostics, and biosensing (Yang et al. 2012). To assess this, the GSH-capped QDs were incubated in three solvent systems Milli-Q water, PBS, and full DMEM medium at room temperature for seven days. The QDs exhibited remarkable stability in Milli-Q water, with a fluorescence intensity reduction of less than 10% and an insignificant increase in hydrodynamic diameter. This signified negligible aggregation or surface deterioration. In PBS, minor alterations were noted; fluorescence intensity decreased by approximately 20% throughout the 7-day duration, and the average particle size rose from ~11.2 nm to ~15–18 nm, indicating mild salt-induced aggregation. In DMEM, the most intricate media comprising serum proteins and amino acids, a notable decrease in fluorescence (~40%) was seen, along with an increase in hydrodynamic size to around ~30 nm, indicating strong interaction with biomolecules as shown in Fig 5.

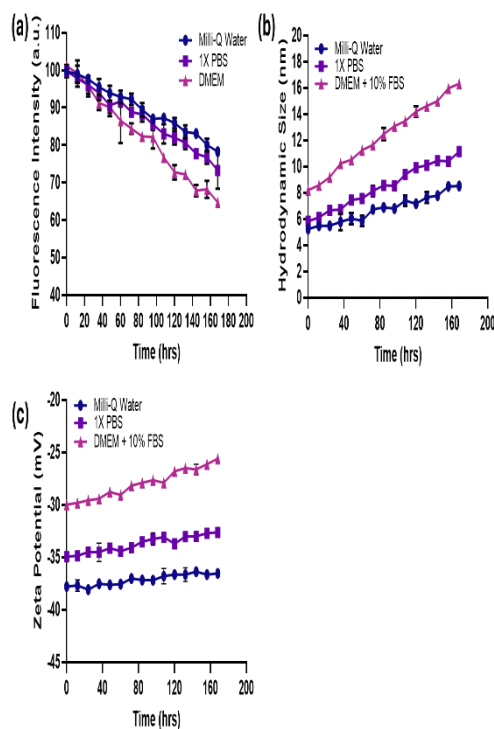


**Fig 5.** Stability profile of CdS/ZnS/GSH QDs in different solvents over a 7-day period. (a) Fluorescence intensity normalized to day 0 shows superior optical stability in Milli-Q water, followed by PBS and DMEM. (b) Hydrodynamic diameter increases over time, particularly in DMEM, suggesting aggregation. (c) Zeta potential values indicate highest colloidal stability in Milli-Q water due to more negative surface charge, with diminished stability in PBS and DMEM.

Zeta potential measurements validated these tendencies, with values diminishing sequentially from -25 mV (water) to -18 mV (PBS) and -12 mV (DMEM), respectively. These data align with the concept that protein adsorption and ionic shielding diminish surface charge and facilitate weak aggregation. Nonetheless, despite these changes, the particles maintained a stable suspension without observable precipitation, suggesting that

GSH imparts significant stability even in intricate biological contexts. This endorses its ongoing employment for short-term biological uses and suggests the possibility of further surface modifications, such as PEGylation, to enhance stability in in vivo environments (Balavandy et al. 2014).

### 3.5. pH-Responsive Colloidal and Optical Properties

The pH-dependent stability of GSH-capped QDs was examined to replicate several physiological and storage circumstances (Li et al. 2017). Samples were cultured in buffers with pH values between 4.0 and 9.0, and their optical and colloidal properties were observed over a period of seven days. At physiological pH (7.0–7.5), the QDs retained more than 90% of their initial fluorescence and exhibited a consistent hydrodynamic size of approximately 12–13 nm. At this pH, the zeta potential was at its highest negative (-25 to -28 mV), indicating excellent electrostatic repulsion and colloidal dispersion. Under acidic circumstances (pH 4.0–5.5), a substantial reduction in fluorescence (~40–50%) was noted, accompanied by a marked increase in particle size to ~25–30 nm. The reduction in zeta potential to approximately -12 mV signified the protonation of carboxylate and thiol groups, hence diminishing ligand–metal interaction and facilitating aggregation. Acidic conditions can result in partial shell disintegration (e.g., ZnS degradation), hence augmenting surface defect states and nonradiative recombination, which diminishes photoluminescence as shown in Fig 6.

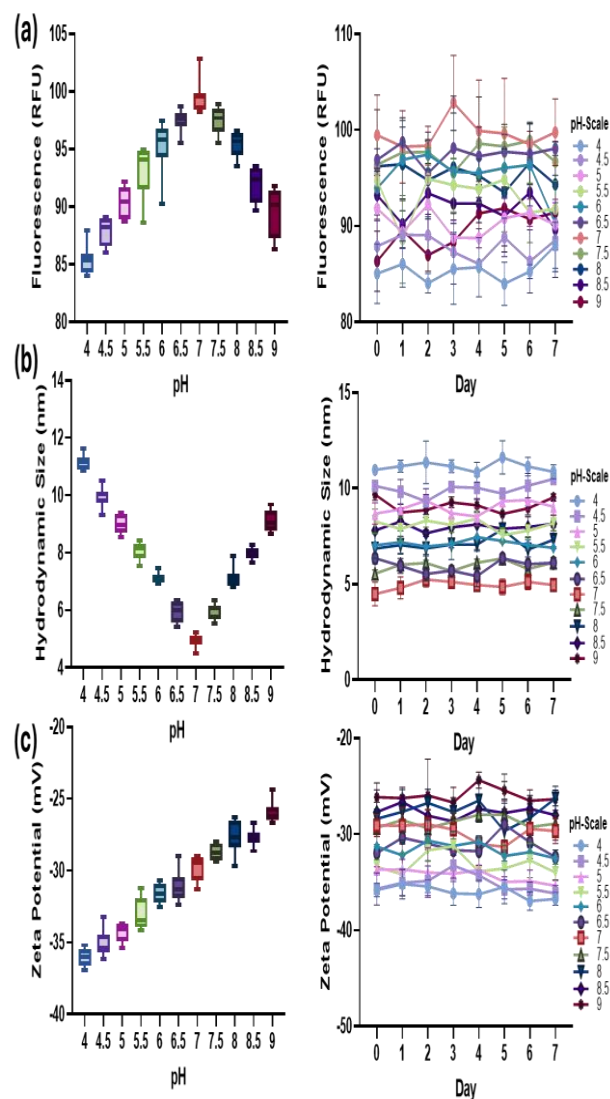


**Fig 6.** Stability analysis of CdS/ZnS/GSH QDs in citrate, phosphate, and borate buffers (pH 4.0 to 9.0) over 7 days. (a) Fluorescence intensity demonstrates optimal optical stability at pH 7.0–7.5, with degradation under acidic conditions. (b) Hydrodynamic diameter increases under extreme pH due to aggregation, with minimal change at neutral pH. (c) Zeta potential reveals highest colloidal stability in neutral and mildly basic buffers, correlating with sustained dispersion.

In basic buffers (pH 8.5–9.0), a considerable decrease in fluorescence

(~20–25%) and a slight increase in size (15–18 nm) were observed. Zeta potential readings were moderately negative (–20 mV), indicating partial deprotonation of surface functional groups and enhanced charge stability. The QDs exhibited excellent stability in neutral to moderately basic pH ranges, aligning with physiological conditions, and shown diminished performance under acidic stress, which may occur in lysosomes or acidic tissue microenvironments. These findings underscore the significance of pH adjustment in the development of QD-based delivery systems or biosensors (Wu et al. 2020).

### ***3.6 Consequences and Comparative Analysis with Existing Literature***

The stability trends identified in this work correspond closely with earlier publications highlighting the significance of thiol-based ligands in preserving nanoparticle integrity in aqueous environments. Research conducted by García, et al. (2014) has emphasized the zwitterionic nature of GSH as a pivotal element in reducing non-specific protein adsorption and aggregation (García et al. 2014). The documented persistence of photoluminescence and size maintenance in our data corroborates this concept. Furthermore, prior research by Zhang et al. (2017) demonstrated that thiol-metal coordination imparts both thermodynamic and kinetic stability to semiconductor nanocrystals, inhibiting surface oxidation and defect development (Zhang et al. 2017). The capacity of GSH to maintain a negative surface charge in diverse media further validates its role as a stabilizing

agent. Although acidic pH undermines stability, this is an acknowledged constraint of most thiol-capped systems and may be mitigated by integrating supplementary protective layers or pH-responsive shielding agents in forthcoming formulations.

### **4. Conclusions**

This study demonstrates that reduced glutathione is an exceptionally effective ligand for transforming hydrophobic CdS/ZnS QDs into stable, water-dispersible nanostructures. The successful ligand exchange was validated by FTIR spectral evidence of thiol-metal coordination and amide vibrations specific to glutathione. Dynamic light scattering indicated a slight increase in hydrodynamic size post-capping, whereas zeta potential tests showed a substantial enhancement in electrostatic stability in aqueous solutions. The GSH-functionalized QDs demonstrated exceptional colloidal and optical stability in pure water and physiologically relevant pH buffers, preserving particle size and fluorescence for seven days. Protein-rich environments, such as DMEM, resulted in partial aggregation and reduced emission intensity, underscoring the influence of serum components on nanoparticle behaviour. The results indicate that GSH-capped QDs are ideal for short-term aqueous or in vitro applications and provide a dependable foundation for subsequent surface functionalization in targeted diagnostic or therapeutic systems.

### **Acknowledgements**

The authors express their gratitude to the Department of Biotechnology, Faculty of Science, Osmania University, Hyderabad, for its institutional assistance during this project. Gratitude is expressed to the Centre for Nano and Soft Matter Sciences (CeNS), Bengaluru, for providing access to cutting-edge instrumentation facilities that facilitated the advanced characterisation of the QDs. We applaud Denisco Chemicals Pvt. Ltd., Hyderabad, for enabling the synthesis and material processing of CdS/ZnS and CdS/ZnS/GSH QDs. Their inputs were important in finalizing the experimental work detailed in this publication.

### Disclosure Statement

The authors declare that there are no conflicts of interest or financial relationships that could have appeared to influence the work reported in this study.

### Author Contributions

Rama Siripelly conducted the experimental work, including synthesis, characterization, data acquisition, and analysis. Anupalli Roja Rani conceived the study, supervised the research, interpreted the results, and contributed to manuscript writing and editing. Both authors read and approved the final version of the manuscript. Anupalli Roja Rani is the corresponding author for this publication.

### Funding Statement

This research did not receive any specific grant from funding agencies in the public, commercial, or not-for-profit sectors. However, the work was supported by

institutional resources provided by the Department of Biotechnology, Faculty of Science, Osmania University, Hyderabad.

### Ethical Approval Statement

This study does not involve any experiments on humans or animals. Therefore, ethical approval was not required.

### References

1. Al-Barram LF (2021) Laser enhancement of cancer cell destruction by photothermal therapy conjugated glutathione (GSH)-coated small-sized gold nanoparticles. *Lasers in Medical Science* 36 (2):325-337
2. Amiri Z, Taromi P, Alavi K, Ghahramani P, Cho WC, Farani MR, Huh YS (2025) Quantum Dot-Infused Nanocomposites: Revolutionizing Diagnostic Sensitivity. *Nanoscale*
3. Bagherpour S, Pérez-García L (2024) Recent advances on nanomaterial-based glutathione sensors. *Journal of Materials Chemistry B*
4. Balavandy SK, Shameli K, Biak DRBA, Abidin ZZ (2014) Stirring time effect of silver nanoparticles prepared in glutathione mediated by green method. *Chemistry Central Journal* 8 (1):11
5. Chakrabarty S, Maity S, Yashini D, Ghosh A (2020) Surface-directed disparity in self-assembled structures of small-peptide l-glutathione on gold and silver nanoparticles. *Langmuir* 36 (38):11255-11261
6. García KP, Zarschler K, Barbaro L, Barreto JA, O'Malley W, Spiccia L, Stephan H, Graham B (2014) Zwitterionic-coated "stealth" nanoparticles for biomedical applications: recent advances in countering biomolecular corona formation and uptake by the mononuclear phagocyte system. *Small* 10 (13):2516-2529
7. Jiang C, Zhang C, Song J, Ji X, Wang W (2021) Cytidine-gold nanoclusters as

- peroxidase mimetic for colorimetric detection of glutathione (GSH), glutathione disulfide (GSSG) and glutathione reductase (GR). *Spectrochimica Acta Part A: Molecular and Biomolecular Spectroscopy* 250:119316
8. Kaur P, Gadhave K, Garg N, Deb D, Choudhury D (2021) Probing the interaction of glutathione with different shape of silver-nanoparticles by optical spectroscopy. *Materials Today Communications* 26:102137
  9. Koo SH, Lee J-S, Kim G-H, Lee HG (2011) Preparation, characteristics, and stability of glutathione-loaded nanoparticles. *Journal of Agricultural and Food Chemistry* 59 (20):11264-11269
  10. Li Y, Zhi X, Lin J, You X, Yuan J (2017) Preparation and characterization of DOX loaded keratin nanoparticles for pH/GSH dual responsive release. *Materials Science and Engineering: C* 73:189-197
  11. Liao C, Li Y, Tjong SC (2019) Bactericidal and cytotoxic properties of silver nanoparticles. *International journal of molecular sciences* 20 (2):449
  12. Martynenko I, Litvin A, Purcell-Milton F, Baranov A, Fedorov A, Gun'Ko Y (2017) Application of semiconductor quantum dots in bioimaging and biosensing. *Journal of Materials Chemistry B* 5 (33):6701-6727
  13. Mondal J, Lamba R, Yukta Y, Yadav R, Kumar R, Pani B, Singh B (2024) Advancements in semiconductor quantum dots: expanding frontiers in optoelectronics, analytical sensing, biomedicine, and catalysis. *Journal of Materials Chemistry C* 12 (28):10330-10389
  14. Sahu M, Ganguly M, Doi A (2024) Role of glutathione capping on copper nanoclusters and nanoparticles: A review. *Journal of Cluster Science* 35 (6):1667-1685
  15. Santos MdC, Seabra A, Pelegrino M, Haddad P (2016) Synthesis, characterization and cytotoxicity of glutathione-and PEG-glutathione-superparamagnetic iron oxide nanoparticles for nitric oxide delivery. *Applied Surface Science* 367:26-35
  16. Shao L, Gao Y, Yan F (2011) Semiconductor quantum dots for biomedical applications. *Sensors* 11 (12):11736-11751
  17. Vyshnava SS, Pandluru G, Kumar KD, Panjala SP, Banapuram S, Paramasivam K, Devi KV, Anupalli RR, Dowlatabad MR (2022) Quantum dots based in-vitro co-culture cancer model for identification of rare cancer cell heterogeneity. *Scientific reports* 12 (1):5868
  18. Wu W, Chen M, Luo T, Fan Y, Zhang J, Zhang Y, Zhang Q, Sapin-Minet A, Gaucher C, Xia X (2020) ROS and GSH-responsive S-nitrosoglutathione functionalized polymeric nanoparticles to overcome multidrug resistance in cancer. *Acta biomaterialia* 103:259-271
  19. Yadav R, Preet S (2023) Comparative assessment of green and chemically synthesized glutathione capped silver nanoparticles for antioxidant, mosquito larvicidal and eco-toxicological activities. *Scientific Reports* 13 (1):8152
  20. Yang J, Zhang W-H, Hu Y-P, Yu J-S (2012) Aqueous synthesis and characterization of glutathione-stabilized  $\beta$ -HgS nanocrystals with near-infrared photoluminescence. *Journal of colloid and interface science* 379 (1):8-13
  21. Yang Z, Lyu J, Qian J, Wang Y, Liu Z, Yao Q, Chen T, Cao Y, Xie J (2025) Glutathione: a naturally occurring tripeptide for functional metal nanomaterials. *Chemical Science* 16 (16):6542-6572
  22. Zhang S, Geryak R, Geldmeier J, Kim S, Tsukruk VV (2017) Synthesis, assembly, and applications of hybrid nanostructures for biosensing. *Chemical reviews* 117 (20):12942-13038